Atmos. Chem. Phys. Discuss., 13, 29895–29945, 2013
www.atmos-chem-phys-discuss.net/13/29895/2013/
doi:10.5194/acpd-13-29895-2013


Atmospheric Chemistry and Physics Discussions



# Assessment of uncertainties of an aircraft-based mass-balance approach for quantifying urban greenhouse gas emissions

**M. O. Cambaliza[1], P. B. Shepson[1,2], D. Caulton[1], B. Stirm[3], D. Samarov[5], K. R. Gurney[9], J. Turnbull[6], K. J. Davis[4], A. Possolo[5], A. Karion[7,8], C. Sweeney[7,8], B. Moser[1], A. Hendricks[1], T. Lauvaux[4], K. Mays[1], J. Whetstone[5], J. Huang[9], I. Razlivanov[9], N. L. Miles[4], and S. J. Richardson[4]**

[1]Department of Chemistry, Purdue University, West Lafayette, IN, USA
[2]Department of Earth, Atmospheric and Planetary Science and Purdue Climate Change Research Center, Purdue University, West Lafayette, IN, USA
[3]Department of Aviation Technology, Purdue University, West Lafayette, IN, USA
[4]Department of Meteorology, The Pennsylvania State University, University Park, PA, USA
[5]National Institute of Standards and Technology, Gaithersburg, MD, USA
[6]National Isotope Centre, GNS Science, Lower Hutt, New Zealand
[7]University of Colorado, Boulder, CO, USA
[8]NOAA Earth System Research Laboratory, Boulder, CO, USA







[9]School of Life Sciences, Arizona State University, Tempe, AZ, USA

Received: 23 July 2013 – Accepted: 24 October 2013 – Published: 14 November 2013

Correspondence to: M. O. Cambaliza (mcambali@purdue.edu)

Published by Copernicus Publications on behalf of the European Geosciences Union.





ACPD
13, 29895–29945, 2013



## Abstract

Urban environments are the primary contributors to global anthropogenic carbon emissions. Because much of the growth in $CO_2$ emissions will originate from cities, there is a need to develop, assess and improve measurement and modeling strategies for quantifying and monitoring greenhouse gas emissions from large urban centers. In this study the uncertainties in an aircraft-based mass balance approach for quantifying carbon dioxide and methane emissions from an urban environment, focusing on Indianapolis, IN, USA, are described. We investigate the uncertainties in our aircraft-based mass balance approach by (1) assessing the sensitivity of the measured flux to important measurement and analysis parameters including wind speed, background $CO_2$ and $CH_4$, boundary layer depth, and interpolation technique, and (2) determining the flux at two or more downwind distances from a point or area source in rapid succession, assuming that the emission flux is constant. When we quantify the precision in the approach by comparing the estimated emissions derived from measurements at two or more downwind distances from an area or point source, we find that the minimum and maximum repeatability were 12 % and 52 %, with an average of 31 %. We suggest that improvements in the experimental design can be achieved by careful determination of the background concentration, monitoring the evolution of the boundary layer through the measurement period, and increasing the number of downwind horizontal transect measurements at multiple altitudes within the boundary layer. Here we also discuss the potential application of the aircraft-based mass balance approach to megacities.

## 1 Introduction

The persistent and uncertain future consequences of global climate change are principally driven by the addition of greenhouse gases to the atmosphere. Although a brief decline in global fossil fuel emissions due to the recent global financial crisis in 2009 was observed, the following year saw a steep rebound in emissions that reached





ACPD
13, 29895–29945, 2013



a record high of approximately 9.1 ± 0.5 petagrams of carbon (Pg C) (Peters et al., 2012). This value combined with emissions from land-use change (0.9 ± 0.7 Pg C) results in a total 2010 anthropogenic emission estimate of 10.0 ± 0.9 Pg C (Peters et al., 2012). Relative to pre-industrial concentrations, the present day increases in atmospheric $CO_2$ and $CH_4$, two of the most important anthropogenic greenhouse gases, have a combined radiative forcing of $\sim 2.1\,W\,m^{-2}$ in 2005 or about 81 % of the anthropogenic forcing from total long-lived greenhouse gases (Forster et al., 2007).

The global fossil fuel $CO_2$ emission is considered to be well known, but uncertainties are growing because of increasing contributions from emerging economies (Gregg et al., 2008; Marland, 2008; Peters et al., 2012). Whereas the uncertainty in fossil fuel emissions from the United States and European countries is estimated to be on the order of 3–5 % (Marland, 2012), recent findings using national and aggregated provincial energy statistics have shown that the uncertainty in fossil fuel $CO_2$ emissions from China is 18 %, which is equivalent to 0.38 Pg C (1.4 gigatonnes of carbon dioxide) (Guan et al., 2012; Marland, 2012) and greater, for example, than Japan's 2008 reported fossil fuel emission (Boden et al., 2011; Marland, 2012).

Considerable uncertainty, from 10 to 40 % between emission inventories, is also observed at the regional level even for countries with relatively stable economies (Peylin et al., 2011). Large uncertainties in fossil fuel emissions were also observed for inventories of geopolitical units smaller than nations (Gurney et al., 2009; Ciais et al., 2010). For example, Gurney et al. (2009) estimate a 16 % uncertainty in the bottom up emission approach at the state level and up to 50 % at the county level in the United States. Considerable differences in flux estimates between bottom-up and top-down approaches have also been reported in the regional (Bergamaschi et al., 2010) and city scales (Mays et al., 2009; Wunch et al., 2009). The magnitude of these uncertainties is such that it calls into question the ability of nations who may commit to mitigation activities to determine the effectiveness of their approaches, e.g., a reduction target of 10 % by 2020 could be difficult to substantiate with such uncertainty levels.





ACPD
13, 29895–29945, 2013



Human activities are focused in and around cities where the majority of the energy produced for electricity and transportation is consumed. In the coming decades, cities will be critical in the global effort to both mitigate and adapt to the consequences of climate change. By 2030, approximately 74 % of $CO_2$ worldwide is predicted to be emitted from cities (World Bank, 2010; IEA Report, 2008), and in the US, that figure is 87 %. Approaches must be in place to verify compliance to future emissions mitigation agreements, preferably those based on atmospheric measurements. McKain et al. (2012) suggest that remote sensing methods such as column observations from satellite or ground-based measurements are ideal approaches for detecting emission trends from urban environments. More recently, Kort et al. (2012) demonstrated the potential of satellite-based measurements to distinguish fossil fuel signals from megacities relative to background regions for long-term monitoring of emission trends, but also mentioned the need for other methods to support and validate space-based retrievals.

Here, we describe and evaluate an aircraft-based mass balance approach for quantifying fossil fuel emissions in urban environments using Indianapolis, Indiana as a case study. This study is part of the Indianapolis Flux Experiment (INFLUX), a multi-institution collaborative project that aims to develop, assess and improve bottom-up and top-down approaches for quantifying greenhouse gas emissions from urban environments using Indianapolis as a case study. As part of INFLUX, there are currently twelve instrumented towers in Indianapolis that are monitoring the abundances of greenhouse gases using in-situ cavity ring-down spectroscopy and flask sampling (http://influx.psu.edu). Aside from the aircraft-based mass balance approach, tower and aircraft in-situ and flask data will be combined with inverse modeling to independently estimate the $CO_2$ and $CH_4$ emissions from Indianapolis. Results from these top-down approaches will be compared with the Hestia bottom-up approach (Gurney et al., 2012).

Aircraft-based mass balance methods have been used to quantify the emissions from urban regions (Kalthoff et al., 2002; Mays et al., 2009; Trainer et al., 1995; Turnbull et al., 2011) as well as from point and area sources (Karion et al., 2013b; Pieschl et al.,





ACPD
13, 29895–29945, 2013



2013; Ryerson et al., 2001; Walter et al., 2012; Wratt et al., 2001). In this work, we investigate the uncertainty of an aircraft-based mass balance approach for estimating urban fluxes by: (1) assessing the sensitivity of the estimated city-wide $CO_2$ and $CH_4$ fluxes for several flight experiments due to the uncertainties in the measurement and analysis parameters, i.e., regional background concentration of $CO_2$ and $CH_4$, depth of the convective boundary layer, magnitude of the perpendicular wind speed, and choice of the interpolation technique used in the mass balance calculations; and (2) determining the flux at two or more downwind distances from a point or area source in rapid succession, assuming that the emission rate is constant.

A total of seven flight experiments were analyzed in this study. In the methods, and results and discussion sections, we describe and discuss in detail the (1) experimental flight plan, and flux calculations, (2) three Indianapolis flight experiments that were used in the sensitivity analyses, and (3) four flight experiments downwind of relatively strong $CO_2$ and $CH_4$ emitters (a power generating station and two landfills) to assess the precision of the approach. From our analyses, we identify the most important parameters that affect the flux, and use these insights to recommend improved experimental approaches for urban area-wide aircraft-based flux measurements.

## 2 Methods

### 2.1 Site description and bottom up data

As of the recent 2010 census, Indianapolis (39.79° N, 86. 15° W, Fig. 1) is the twelfth most populous city in the United States (www.census.gov, accessed 9 April 2012). The city of Indianapolis is an ideal test area for evaluating and improving measurement strategies for quantifying urban-scale fossil fuel emissions. Indianapolis is sufficiently removed from other metropolitan areas and is surrounded by cropland so that its fossil fuel signal above background should be relatively easily identified. It is also characterized by flat terrain, making the meteorology relatively simple. The Vulcan high resolu-





ACPD
13, 29895–29945, 2013



tion data product (Gurney et al., 2009) shows that the fossil fuel $CO_2$ emission rate from Marion county (equivalent to the city of Indianapolis) in 2002 was $\sim 3.6\,\mathrm{Mt\,C\,yr^{-1}}$, providing a relatively large signal that can be easily detected by aircraft and tower-based measurement systems (see also http://vulcan.project.asu.edu). More recently, Gurney et al. (2012) quantified all fossil fuel emissions from Indianapolis at much finer spatial and temporal scales down to the building and street levels, at hourly time scales, for year 2002 (see also http://hestia.project.asu.edu). This comprehensive downscaling study provides an independent estimate of the fossil fuel $CO_2$ flux from the city to which we will compare emission estimates from top-down approaches such as the aircraft-based mass balance method presented here.

### 2.2 Aircraft-based measurements of greenhouse gases and meteorological parameters

Several flight experiments were conducted in 2011 downwind of Indianapolis, IN using Purdue University's Airborne Laboratory for Atmospheric Research (http://www.chem.purdue.edu/shepson/alar.html). The aircraft platform is a Beechcraft Duchess, a modified twin-engine aircraft with a compartment space of $\sim 1\,\mathrm{m^3}$ for instrumentation. It is equipped with (1) a global positioning and inertial navigation system (GPS/INS), (2) a Best Air Turbulence (BAT) probe for wind measurements (Garman et al., 2006), (3) a cavity ring-down spectroscopic system for real-time, in-situ measurement of greenhouse gas concentrations (Crosson et al., 2008; Karion et al., 2013a), (4) an in-flight $CO_2/CH_4$ calibration system, and (5) a Programmable Flask Package for discrete sampling of ambient air.

Concentrations of methane, carbon dioxide and water were measured at a frequency of 0.5 Hz using an in-situ flight-ready Picarro cavity ring-down spectrometer (CRDS) model number G2301-*f* (Crosson, 2008; Chen et al., 2010; Karion et al., 2013a). Ambient air from the nose of the aircraft was pulled through a 5 cm diameter PFA Teflon tube at a flow rate of $1840\,\mathrm{L\,min^{-1}}$ (equivalent to a $\sim 0.1$ s residence time) using a blower installed at the rear of the aircraft. The CRDS was connected to the Teflon tubing via





ACPD
13, 29895–29945, 2013



a "T" connection, pumping air continuously through the analyzer. Because the flow rate through the analyzer is 450 standard mL $min^{-1}$, the time required to purge the sampling system was determined to be ~ 6.7 s. Inflight calibrations for $CO_2$ and $CH_4$ were achieved using a valve-switching calibration system and three NOAA/ESRL reference cylinders with the following mole fractions: 378.49, 408.83, and 438.29 ppm for $CO_2$, and 1803.0, 2222.2, and 2599.5 ppb for $CH_4$, respectively (Dlugokencky et al., 2005; Zhao and Tans, 2006). Figure S1a and b (Supplement) shows inflight calibration curves for $CO_2$ and $CH_4$ for several flight experiments, showing excellent reproducibility of the indicated concentrations over five months (near zero drift), and good linearity. The measurement precision for $CO_2$ and $CH_4$ during inflight calibrations was 0.1 ppm and 2.6 ppb, respectively. Residuals from the fit ranged from −2.6 ppb to 3.9 ppb for $CH_4$ and from −0.1 to 0.2 ppm for $CO_2$.

In addition to in-situ spectroscopic measurements of $CO_2$ and $CH_4$ mole fractions, discrete grab samples of ambient air were obtained using the Programmable Flask Package (PFP), which were later analyzed at NOAA for a suite of trace gases (~ 55 species) (methods described in http://www.esrl.noaa.gov/gmd/ccgg/aircraft/packages.html). The PFP consists of twelve 700 mL glass flasks that are pressurized to 2.7 atmospheres. Figure S2 (Supplement) shows excellent linearity ($R^2$ = 0.99) with slopes identical to unity at 95 % CL (confidence level) between the $CO_2$ and $CH_4$ concentrations obtained from continuous measurements with the CRDS and grab sampling with the PFP for several flight experiments. To obtain enough air for radiocarbon measurements, two flasks were filled simultaneously (Turnbull et al., 2011). The first flask was analyzed for greenhouse gases, hydrocarbons and halocarbons, as well as stable isotopes of carbon dioxide and methane ($\delta^{13}CO_2$, $\delta^{13}CH_4$) (methods and calibration scales described in http://www.esrl.noaa.gov/gmd/ccl/scales.html; Montzka et al., 1993; Vaughn et al., 2004). The second flask was dedicated for $^{14}CO_2$ measurement (Turnbull et al., 2007). Previous work (Turnbull et al., 2011) has shown that there is no significant difference in trace gas mixing ratios between the two simultaneously filled flasks.





ACPD
13, 29895–29945, 2013



To investigate any potential systematic bias in the concentration measurements, we estimate the concentration measurement uncertainty as the average difference between the CRDS measurements and the $CO_2$ and $CH_4$ mole fractions simultaneously obtained from discrete flask sampling (Fig. S2, Supplement). The $CO_2$ and $CH_4$ concentrations in flask samples were determined using non-dispersive infrared analysis (NDIR) (Conway et al., 1994; see also method description in http://www.esrl.noaa.gov/gmd/ccgg/aircraft/analysis.html, accessed 21 February 2013) and gas chromatography (GC) (Dlugokencky et al., 1994), respectively. We find that the relative differences between the CRDS and flask measurements are randomly distributed about zero for both $CO_2$ and $CH_4$ (Fig. S3, Supplement). On the basis of this analysis, there is no apparent systematic bias in the CRDS measurements.

Wind vectors were measured at 50 Hz using the BAT probe, a nine-port pressure probe extending from the nose of the aircraft (Garman et al., 2006, 2008). The measured pressure differentials across the hemisphere of the probe are combined with 50-Hz inertial information from the GPS/INS system to yield the 3-D wind distribution. The accuracy in the horizontal wind measurements was determined by Garman (2009) to be $\pm 0.4\ ms^{-1}$. At the center of the hemisphere is a microbead thermistor for ambient temperature measurements.

### 2.3 Experimental flight design

The experimental flight design was discussed in full detail by Mays et al. (2009). In summary, flight experiments were conducted between 11:00 LT and 16:00 LT when the boundary layer was essentially fully developed. Prior to each flight experiment, the prevailing wind direction was estimated using the Hybrid Single Particle Lagrangian Integrated Trajectory Model (HYSPLIT, Draxler and Rolph, 2012). The aircraft heading was such that the ground track was perpendicular to the wind direction determined from the HYSPLIT back trajectory at 500 m a.g.l. (above ground level), and from surface wind reports in-flight. Constant altitude horizontal transects were conducted downwind of Indianapolis at various altitudes up to the top of the convective boundary layer. The city of





ACPD
13, 29895–29945, 2013



Indianapolis is about 70 km wide, and each horizontal transect was ~ 90 to 100 km long so that regional background concentrations of methane and carbon dioxide could be estimated from the edges of the transects. By flying perpendicular to the wind direction on level flight paths at multiple altitudes in the boundary layer, the aircraft intercepted and detected elevated concentrations of $CO_2$ and $CH_4$ directly downwind of anthropogenic sources from the urban environment in a two-dimensional plane. Two to three hours of flight time were used to generate a rastered 2-D vertical plane. Given a typical aircraft speed of 70 m s$^{-1}$ and CRDS measurement frequency of 0.5 Hz, the horizontal resolution within the plane was 140 m. The depth of the convective boundary layer (CBL) was determined from vertical profile measurements of water, potential temperature, and variance of the vertical wind speed, during which the aircraft ascended and descended in a spiral path from the surface up to a height of ~ 4000 m a.g.l. in the free troposphere.

Figure 1 shows, for example, the flight path as a function of altitude downwind of Indianapolis on 1 June 2011. The black outline shows the city boundary of Indianapolis based on the 2010 US Census population density of an urbanized area (http://www.census.gov/geo/reference/ua/urban-rural-2010.html, accessed 26 November 2012), which encloses regions that have population densities of ≥ 390 people km$^{-2}$. For this particular experiment, two sets of vertical profiles were performed, before and after the horizontal transects. The location of carbon dioxide and methane sources such as power generating facilities, an incineration plant, landfills, and wastewater treatment plants within and outside the city limits are also shown in the figure. We note that the Harding Street power plant (HSPP) and the Southside Landfill, the largest $CO_2$ and $CH_4$ sources in Indianapolis, respectively, are almost co-located in the southwest side of the city, separated only by a distance of about 1 km. The brown outline shows the major highways and arterial roads that traverse into and around the city.





ACPD
13, 29895–29945, 2013



## 2.4 Flux calculation

The flux or mass flow rate of species $C$ through a crosswind plane downwind of the city is estimated by the integration of the enhancement above the background concentration $[C]_b$ combined with the component of the wind perpendicular to the plane (Trainer et al., 1995; White et al., 1983), as shown in Eq. (1).

$$F = \int_0^{z_i} \int_{+x}^{x} ([C] - [C]_b) \times U_\perp \, dx \, dz \quad (1)$$

In Eq. (1), $z_i$ is the depth of the convective boundary layer, $-x$ and $+x$ are the horizontal limits of the plume width from an arbitrary midpoint.

In our analysis, the observed horizontal flight distributions for $CH_4$, $CO_2$, temperature, pressure and perpendicular wind speeds were interpolated in a two-dimensional gridded plane using a kriging approach (Matlab-based EasyKrig3.0, Chu, 2010). We use a 10 s running average of the 50-Hz perpendicular wind speed to obtain the magnitude of the sustained winds at each altitude. During interpolation, a semivariogram of the data is calculated and modeled using the variogram model specified in Eq. (1) of Mays et al. (2009). The parameters of the model (power, nugget, sill, range and length) are adjusted to achieve an optimum fit to the empirical semivariogram of the data. The quality of the interpolation is assessed using the Q1 (distribution of the deviation for the mean) and Q2 (distribution of deviations for the standard deviation) criteria (Chu, 2010). The raw data were interpolated using a 20 m by 200 m kriging resolution in the vertical and horizontal directions, respectively.

Using the measured mean wind direction, the edges of the city are projected onto the horizontal transect to define the $-x$ and $+x$ horizontal limits of integration. The section in the transect outside the projected city limits is used to calculate the mean background concentration $\left[\bar{C}\right]_b$, which was then subtracted from the gridded 2-D concentrations, $[C]_{xz}$, to obtain the enhancement from the city plume. The net molar concentration at each grid cell (mol m$^{-3}$) was then determined from the ideal gas law, and





ACPD
13, 29895–29945, 2013



the interpolated pressure and temperature distributions. This incremental concentration was subsequently multiplied by the mean component of the gridded wind speed perpendicular to the 2-D plane $(\bar{U}_{\perp})$, calculated at each altitude, to determine the net flow of molecules across each grid cell. Finally, the city-wide emission flux, $F$ (mol s$^{-1}$), was calculated by integrating the net perpendicular molecular flow over the vertical and horizontal dimensions as described in Eq. (1). In this relationship, d$x$ and d$z$ are the horizontal and vertical grid spacing (m) corresponding to the kriging resolution of 200 m and 20 m, respectively, $[\bar{C}]_b$ is the mean background molar concentration, and $-x$ and $+x$ are the effective horizontal boundaries of the city determined from projecting the city limits onto the horizontal transect plane. We refer to this analysis method as the multi-transect kriging approach.

### 2.5 Sensitivity analyses

To develop an understanding of the relative importance of factors influencing the flux measurement uncertainty, we conducted a sensitivity analysis of the multi-transect kriging approach. Three flight experiments downwind of Indianapolis conducted on 1 March, 29 April, and 1 June 2011 were considered for these analyses. We investigate the magnitude of the change in the flux as a function of the uncertainties of three parameters: background $CO_2$ and $CH_4$, depth of the convective boundary layer, and perpendicular wind speed. We also quantified the change in the flux as a function of the choice of interpolation method, which is a form of model uncertainty (Clyde and George, 2004).

The background concentrations were obtained from the edges of the gridded two-dimensional $CO_2$ and $CH_4$ matrices outside the city boundaries. We examined the influence of the background on the estimated flux in two ways. First, we compared the resulting flux using a vertically varying background, as well as from background concentrations that were averaged over the boundary layer. We determined the vertical distribution of the background (Fig. S4, Supplement) by calculating the mean over 20 m altitude bins, which correspond to the kriging resolution in the vertical direction.





ACPD
13, 29895–29945, 2013



Second, we calculated the sensitivity of the flux estimate to the uncertainty in the mean background concentration, i.e., $\Delta\text{Flux}/\Delta b$ where $\Delta$Flux is the change in the flux and $\Delta b$ is the mean background concentration uncertainty, which is a combination of the measurement accuracy and observed background variability. We calculated the standard deviation in the mean background concentration at each altitude using the method described by Lenschow and Stankov (1986) where the variability in the measured parameter was shown to be dependent on the averaging length, and the CBL depth. As described in Sect. 2.2., there is no apparent systematic bias in the CRDS measurements. Thus $\Delta b$ is attributed to the observed variability in the mean background concentrations, where the variability is defined as the standard deviation of the mean background concentration converted to a 95 % CL. The uncertainty in the background is not constant with altitude. The average uncertainties in the $CO_2$ and $CH_4$ mean background concentrations were determined to be 0.3 ppm, 0.2 ppm, 0.5 ppm, and 1.3 ppb, 3.2 ppb, and 2.6 ppb for the 1 March, 29 April, and 1 June 2011 flight experiments, respectively.

To investigate the influence of the uncertainty in the wind speed on the estimated flux, we calculated $\Delta\text{Flux}/\Delta U_{\perp}$, where $\Delta U_{\perp}$ is the uncertainty in the perpendicular wind speed. As stated above, we calculated the mean perpendicular wind speed $\left(\bar{U}_{\perp}\right)$ at each altitude and estimated the variability by determining the standard deviation of the mean using the Lenschow and Stankov method (1986). The calculated systematic uncertainty in the BAT probe for horizontal wind measurements was determined by Garman (2009) to be $0.4\,\text{m}\,\text{s}^{-1}$. We propagated the systematic uncertainty with the calculated variability to obtain the overall measurement uncertainty $\Delta U_{\perp}$ converted to a 95 % CL. We find that the systematic uncertainty was significantly larger than the variability, such that the overall uncertainty in the perpendicular wind speed was determined to be $\sim 0.7\,\text{ms}^{-1}$ for the three flight experiments.

The change in flux due to the uncertainty in the convective boundary layer (CBL) height (height to which data are interpolated) was also investigated. We note that for two of the three flight experiments considered in these analyses (1 March and 29





ACPD
13, 29895–29945, 2013



April 2011 experiments), one vertical profile was flown after the horizontal transects, while two vertical profiles were obtained for the 1 June 2011 flight experiment (before and after the horizontal transects). Figure 2 shows the ascending vertical profiles of potential temperature ($\theta$), its gradient of $\theta$ with altitude ($z$), and $H_2O$. The altitude with the largest rate of change in $\theta$ (i.e., maximum $d\theta/dz$) is considered to be $z_i$, the altitude representing the top of the CBL. The CBL depths were determined to be 525 m, and 1110 m for the 1 March, and 29 April experiments, respectively; and 1310 m, and 1880 m for the 1 June flight experiment before and after the horizontal transects, respectively. Figure S5 shows the corresponding descending vertical profiles of $\theta$ and $H_2O$ while Table S1 summarizes the observed CBL depths for the three flight experiments.

We note that for the 1 June 2011 flight experiment, the depth of the CBL grew considerably (~ 570 m) within the 4 h duration between the beginning and end of the experiment (panels c and d of Fig. 2). Thus, for this particular case, we calculate the base flux using the CBL depth halfway through the horizontal transects. To determine the CBL depth midpoint through the transects, we estimate the change in the CBL depth using the thermodynamic mixed-layer growth method (Stull, 1997)

$$\Delta z = \left[\frac{2}{\gamma}\left[\overline{w'\theta'_s}\right]\Delta t\right]^{\frac{1}{2}} \quad (2)$$

In this relationship, $\Delta z$ is the change in the CBL depth within the elapsed time $\Delta t$, $\gamma$ is the adiabatic lapse rate, and $\overline{w'\theta'_s}$ is the surface sensible heat flux calculated from the observed fluctuations in the vertical winds and potential temperature during the horizontal transects.

Because two aircraft vertical profiles were performed during the 1 June 2011 experiment, it is possible to determine how well the thermodynamic mixed-layer growth model is able to predict the observed CBL depth. Given the measured CBL depth from the first vertical profile (1310 m), and calculating $\Delta z$ using Eq. (2), the predicted CBL depth at the end of the experiment (elapsed time $\Delta t$ =~ 4 h) was ~ 1990 m, which is ~ 6 %





ACPD
13, 29895–29945, 2013



different from the observed CBL depth at that time (1880 m). Using this model, the predicted CBL height halfway through the horizontal transects was 1720 m, the depth to which we evaluate the base flux for the 1 June 2011 flight experiment.

The CBL uncertainty was obtained from the regression plot of the standard deviation of $z_i$ ($\sigma_{zi}$) vs. $z_i$ determined by Davis et al. (1997) from the BOREAS (Boreal Ecosystem–Atmosphere Study) field campaign where the dynamics of the CBL using a lidar system on an aircraft platform was intensively investigated. The high frequency measurements with the lidar system (one $z_i$ measurement every 13 m) allowed for the investigation of the variability of the CBL top over hundreds of kilometers due to updrafts (rising thermals) and downdrafts and the associated cascade of turbulence to smaller scales. $\sigma_{zi}$ vs. $z_i$ were determined for twelve cases of clear-air convection (12 different CBL depths) collected during eight days of BOREAS field campaigns (Fig. 15 in Davis et al., 1997). We evaluate the sensitivity in the estimated flux due to the uncertainty in the CBL depth corresponding to $\sigma_{zi}$ at a 95 % CL, which was determined to be 75 m, 140 m, and 204 m for 1 March, 29 April, and 1 June, respectively.

We also investigated the sensitivity of the flux to the choice of interpolation method. In all calculations of the base flux, the concentrations, perpendicular wind speed, pressure and temperature were interpolated using the kriging method described above (Chu, 2010). To this end, we evaluated the change in the estimated flux when a different interpolation method was used. The alternative method was a version of local polynomial regression (LPR) method (Fan and Gijbels, 1996), an established method for non-parametric regression. This method fits a *p*th order polynomial regression to each point's immediate neighbors, and produces an interpolated value for the point based on the regression. The challenge with the use of LPR is the selection of the size and shape of these neighborhoods. For data with complex distributions exhibiting both fine and coarse features such as obtained from our flight experiments, adaptive neighborhoods were chosen to interpolate the data over the two-dimensional perpendicular plane. Numerous methods exist for selecting these adaptive neighborhoods. For the





ACPD
13, 29895–29945, 2013



analysis presented here, we implemented the Fast Regularization of the Derivative Expectation Operator method (Lafferty and Wasser, 2008; Samarov, 2012).

### 2.6 Investigation of method precision using flux determinations from multiple downwind distances

In this section, we describe our method for determining the precision of the aircraft-based mass balance approach using successive sequential measurement transects for two or more downwind distances from a point or area source. Four flight experiments were considered for these analyses. The flux is calculated using the multi-transect kriging approach and compared for the multiple sets of transects assuming that the emission from the source is constant over the full flux experiment period. To the extent that the emission source strength or the mixing height and turbulence in the boundary layer are not constant, this approach leads to an evaluation of an upper limit of the method precision, as all these changes will contribute to the overall precision of this approach. For point sources, the same experimental approach as described above for Indianapolis was used during the experiments but the horizontal transects were much shorter, as the sources were smaller in areal coverage. This allowed us to sample the plume repeatedly in rapid succession at finer vertical resolutions, thereby improving the representation of the plume during interpolation.

Two flight experiments were conducted at two downwind distances from the Newton County, IN landfill on 16 June 2011 and 3 May 2012. The Newton County landfill received ~2.9 Mt of waste in 2008 for a daily average of ~9500 t per operating day (2008 Indiana Solid Waste Facility Report). It is one of the three largest landfills in the United States (http://www.cnbc.com/id/39382002/America_s_Largest_Landfills, accessed 6 September 2012; http://www.forbes.com/2010/10/13/los-angeles-las-vegas-business-energy-biggest-landfills.html, accessed 6 September 2012).

We also measured the methane enhancements at two downwind distances from the Twin Bridges Landfill (TBLF), Danville, IN, located about 30 km west of Indianapolis on





ACPD
13, 29895–29945, 2013



30 August 2012. For comparison, the Twin Bridges landfill received ∼ 0.72 Mtons of solid waste in 2008, a factor of four smaller than for the Newton County landfill for the same year (2008 Indiana Solid Waste Facility Report).

The $CO_2$ plume was also sampled at three downwind distances from the Harding Street Power Plant (HSPP) station located at the southwest side of Indianapolis on 1 June 2012. This power generating facility emitted 3.2 million metric tons of $CO_2$ in 2010 (http://ghgdata.epa.gov/ghgp/main.do, accessed on 2 September 2012). The Newton County and Twin Bridges landfills as well as the Harding St. power generating station are idealized small area and point sources for testing the precision, as well as the accuracy (given the relatively well-known source strength data for the power plant) of the aircraft-based flux measurement approach. Their relatively large source strengths make the observed methane and carbon dioxide signals considerably enhanced relative to the background. Figure S6 (Supplement) shows the flight paths as a function of downwind distances for the four experiments used in this analysis.

### 2.7 Calculation of the citywide $CO_2$ and $CH_4$ flux from single-transect observations

To examine the viability of a single-transect approach, we also calculated the citywide $CO_2$ and $CH_4$ emission fluxes using each transect independently for the 1 March, 29 April, and 1 June 2011 flight experiments, similar to the approach implemented in previous studies (Pieschl et al., 2013; Turnbull et al., 2011; Trainer et al., 1995; White et al., 1983). We carry out these calculations with the goal of determining the variability of the independently-determined fluxes from each transect for the single-transect approach, and to compare with the results obtained from our multi-transect-kriging method. The single-transect approach assumes that the measured pollutant plume components are uniformly mixed through the boundary layer in the vertical direction, i.e. that the observed incremental $CO_2$ and $CH_4$ concentrations in a given horizontal transect represent those at all altitudes within the boundary layer. This approach is also described by Eq. (1) except that the assumption of a well-mixed boundary layer effectively re-





ACPD
13, 29895–29945, 2013



moves the need to interpolate the data. Using the observed pressure and temperature distributions from the vertical profile, the molar density of air as a function of altitude is calculated, and is subsequently integrated from the ground to the top of the boundary layer. To obtain the citywide flux, the integrated concentration enhancements are then multiplied by the mean perpendicular wind speed for each transect for $CO_2$ or $CH_4$, along the horizontal limits of the projected city boundary. Note that for the case of the 1 June 2011 flight experiment when the CBL depth grew ~ 570 m, we used the CBL depth halfway through the horizontal transects (1720 m) to be consistent with our method in the multi-transect kriging approach described in Sect. 2.5. We further note that the horizontal transects were of variable lengths, and that a transect was considered for single-transect flux calculation if its length covers the projected width of Marion County, which encompasses the bulk of Indianapolis.

## 3 Results and discussion

### 3.1 Horizontal and temporal distribution of carbon dioxide and methane

Our $CO_2$ measurements are impacted by $CO_2$ emissions and uptake from all sources, including fossil fuel $CO_2$ and biological $CO_2$ sources such as biomass burning, biofuel use, respiration and photosynthesis. Fossil fuel $CO_2$ ($CO_{2ff}$) originates from a variety of sources including energy usage related to residential, commercial and industrial building operations, mobile source combustion within and around the city, and point sources, such as power generating stations and incinerators. $CH_4$ is emitted from biogenic sources such as bacterial activity from landfills and wastewater treatment plants, and from anthropogenic sources such as leakage from natural gas infrastructure, and concentrated animal feeding operations (the latter of which do not exist in Indianapolis). Figure 3 shows sample data for the temporal distributions of $CO_2$, $CH_4$ and $H_2O$ along with altitude above ground for the 1 June 2011 experiment. We also indicate in Fig. 3 the CBL depths for the two vertical profiles flown during this experiment, indi-





ACPD
13, 29895–29945, 2013



cating the ∼ 570 m increase in a 4 h time period (Table S1 and Fig. 2). We note that this considerable growth in boundary layer depth is consistent with the observed ∼ 3 K increase in surface temperature indicated by panels c and d in Fig. 2. We also observe in Fig. 3 the presence of temporally coherent elevated concentrations of $CO_2$ and $CH_4$, with enhancements up to ∼ 9 ppm and ∼ 50 ppb above the background, respectively. The large enhancements are co-located in space, as clearly seen in the horizontal and vertical distributions of observed and kriged $CO_2$ and $CH_4$ in Fig. 4. The x-axis in Fig. 4 represents the distance in kilometers of the flight track from an arbitrarily chosen center point on the horizontal transects. The projected city limits, hence the limits of integration in the horizontal direction, were from −35 km (shown by the white broken line in Fig. 4c and d) to +45 km; the horizontal transects for this experiment were just long enough to encompass the city width in the northeastern side (positive distance). Thus, the background $CO_2$ and $CH_4$ were taken from −48 to −35 km (southwestern edge of the transect). Elevated $CO_2$ concentrations outside the city boundary at the edges of the transects were also observed, and are attributed to the Eagle Valley Power Plant (39.488° N, 86.415° W, Martinsville, IN). In a separate flight experiment on 8 February 2011, we detected the $CO_2$ enhancement from Eagle Valley power plant and followed the plume upwind to ascertain the source. These elevated concentrations do not flow into the city, and hence, were not included in the determination of the background. For this case, $CO_2$ concentrations outside the city boundary were attributed to Eagle Valley Power Plant if they were at least three standard deviations greater than the rest of the background, and correlated by back trajectory analysis to the power plant. For the 1 June 2011 experiment, the background $CO_2$ and $CH_4$ (mean ± 1$s_m$), assumed constant with height, were 392.6 ± 0.5 ppm and 1880.6 ± 2.6 ppb, respectively, where $s_m$ is the standard deviation of the mean at 95 % CL determined using the sampling statistics described by Lenschow and Stankov (1986). Figure 4 shows that in comparison to these numbers, the urban plume was captured downwind of the city, and that the observed enhancements were well above the variability of the background concentrations. We followed the source of the elevated concentrations (∼ 9 ppm and ∼ 50 ppb





ACPD
13, 29895–29945, 2013



enhancements mentioned above) downwind of the city during separate in-flight investigations and found that the largest $CO_2$ and $CH_4$ enhancements were originating from the Harding St. power generating facility, and the Southside landfill and/or the natural gas transmission regulating station (TRS) respectively. These three sources are all situated in the southwest side of the city, with the landfill and TRS adjacently located, and separated by ∼ 1 km from the Harding St. power plant across the White River.

### 3.2 City-wide $CO_2$ and $CH_4$ emissions

City-wide $CO_2$ and $CH_4$ emissions are estimated using the mass balance approach on three days: 1 March, 29 April, and 1 June 2011. We note that the aircraft mass balance method determined the net flux out of the city. For all three flight days, we compare the total $CO_2$ flux estimated using the mass balance approach to the Hestia bottom-up data for fossil-fuel $CO_2$, making the assumption that the measured $CO_2$ is comprised solely of fossil fuel $CO_2$ and there is no biogenic $CO_2$ influence. The work of Turnbull et al. (2013), using $\delta^{14}C$ in $CO_2$ to assess the fossil fuel component of the measured $CO_2$, indicates that in the winter (or non-growing seasons) $CO_2$ enhancements are entirely fossil-derived for Indianapolis. Aircraft flask measurements of the fossil fuel $CO_2$ content from the 29 April and 1 June flight experiments support this assumption, showing good correlations between enhancements in total and fossil fuel $CO_2$ with slopes identical to unity within 2 standard deviations of the slope (Fig. S7, Supplement). However, many of the flasks were sampled within the influence of the power plant plume where the fossil fuel component is larger and more dominant than over the larger urban area. Thus, more flask measurements within the urban plume (but outside the power plant plume) will be useful to examine the extent to which the estimated $CO_2$ emission from the city of Indianapolis is strongly dominated by fossil fuel $CO_2$, particularly during the summer growing season. While for 1 March there were no radiocarbon measurements from aircraft flask samples, analysis of tower-based flask samples shows that $CO_2$ enhancements are entirely fossil-fuel-derived in this late winter period in Indianapolis (Turnbull et al., 2013). We note that for the growing season





ACPD
13, 29895–29945, 2013



periods, biosphere exchange of $CO_2$ represents a component of the measurement uncertainty, important to our comparison with the Hestia bottom-up data. In a companion paper (Turnbull et al., 2013), we discuss the partitioning of the urban $CO_2$ enhancement into the fossil and biogenic components in detail. As discussed in that paper, measurements of the background $CO_2$ at the "sides" of the city, at the time of each transect, are likely optimum, for cases when the background has a diurnally varying character, due to biospheric impacts.

Calculated $CO_2$ and $CH_4$ emission fluxes for these dates are presented in Table 1 and Fig. 5. The estimated emissions (Table 1) were calculated using a vertically varying background for the three flight experiments. As mentioned above, we also calculated the flux using an average $CO_2$ and $CH_4$ background (Table S2, Supplement) assumed to be constant with altitude and found a 3 %, 14 %, and 0.2 % difference in the $CO_2$ flux, and 3 %, 3 %, and 10 % difference in the $CH_4$ flux for the 1 March, 29 April, and 1 June experiments, respectively. As shown in Table 1, there is a 9 % and 30 % difference between the emissions estimated with the aircraft-based mass balance approach and the Hestia bottom-up method for 1 March and 29 April 2011, respectively. However, the measured city-wide $CO_2$ emission from observations was greater than the Hestia county estimate by a factor of $\sim 2.1$ for the 1 June 2011 experiment. For comparison, we include in Fig. 5 the Hestia emissions and aircraft-based mass balance measurements in Indianapolis for 2008 (Mays et al., 2009). Table S3 (Supplement) shows the $CO_2$ emissions from the Hestia bottom-up approach and the aircraft-based mass balance measurements corresponding to the 2008 flight experiments (from Mays et al., 2009). We note that Mays et al. (2009) used the same multi-transect kriging method described above. The combined results from the 2008 and 2011 measurements show considerable day-to-day variability, which does not exist in the bottom-up emission data. When the $CO_2$ fluxes were plotted against traffic flow data, Mays et al. (2009) showed that $\sim 57$ % of the variability in the city-wide $CO_2$ emission can be accounted for by mobile combustion sources. Except for city onroad $CO_2$ emissions and $CO_2$ emissions data from power generating facilities, which are measured and reported to





ACPD
13, 29895–29945, 2013



the EPA, Hestia emission estimates rely on the temporally simulated average emission dynamics for the other sectors, which will vary based on hour of the day and day of the week. Hence, one-to-one agreement between the mass balance approach and the bottom-up emission estimate is not necessarily expected for specific hours within individual days. We also note that Hestia only accounts for the fossil fuel $CO_2$ while our approach captures the total $CO_2$ flux from the city. Thus, if the biological component is significant, our comparison may be biased.

We also report the methane flux from the city for the three flight experiments (Table 1) and note that there is also a considerable variability in the day-to-day emissions. This result may be due in part to the fact that one of the largest contributors to the total citywide methane emission is a landfill in the southwest side of the city, and its daily and seasonal emission is variable due to the dependence on temperature, pressure, and available moisture. The methane emission from Indianapolis and its apportionment to various sources is the subject of a separate manuscript (Cambaliza et al., 2013).

### 3.3 Sensitivity analyses

In this section, we quantify the change in the $CO_2$ and $CH_4$ fluxes due to the uncertainties in the analysis parameters. Table 2 summarizes the results from the sensitivity analyses for the 1 March, 29 April, and 1 June 2011 Indianapolis flight experiments. In our analyses it was not assumed, based on our measurements, that the boundary layer at the downwind observational plane was well-mixed, i.e. that the observations from one horizontal transect are a representative sample of a uniform vertical composition for the entire boundary layer. For our flights, a typical distance to significant upwind point sources, e.g. the power plant, was $\sim 10$ km. For this distance, we typically observe considerable variability in the $CO_2$ and $CH_4$ concentrations in the vertical direction. For example, in Fig. 6 one can see the $CO_2$ and $CH_4$ horizontal transect distributions for 29 April 2011. This figure shows enhancements from $\sim +4$ km to $\sim +8$ km for the 280 m and from $\sim +4$ km to $+16$ km for the 360 m transects, respectively, that are not observed in the other transects. For this sampling day for which the CBL depth





ACPD
13, 29895–29945, 2013



is 1100 m, the characteristic time scale for air to cycle once from the bottom to the top of the CBL (Stull, 1997) is ~ 10 min where the calculated convective velocity scale is ~ 1.9 m s$^{-1}$. The corresponding horizontal length scale for this one cycle time is ~ 2.4 km given that the mean wind speed for this day was ~ 4 m s$^{-1}$. A typical sampling distance of 10 km from the power generating station is approximately four times longer than the 2.4 km length scale. This sampling distance may be sufficient to achieve well-mixed conditions for this point source but the city covers a large area with distributed sources that may be located closer to the horizontal transects. Thus, multiple horizontal transects at various altitudes within the stationarity time constraints (i.e. time intervals in which it is safe to assume unchanging fluxes, CBL depths and winds) are therefore important for accurate sampling of source-specific features. However, it is not possible to sample very close to the ground, and sometimes not possible to sample all the way to the top of the boundary layer; in addition, the vertical spacing between the horizontal transects may be appreciable. For these reasons, there is significant uncertainty resulting from the interpolation procedure (Table 2).

The CBL depths used for the calculations were 525 m, 1110 m, and 1720 m, while the standard deviation of $z_i$ at 95 % CL were 75 m, 140 m, and 204 m for 1 March, 29 April, and 1 June, respectively. Thus, we evaluated the change in the flux corresponding to a relative increase in the CBL depths of 14 %, 13 %, and 12 % for the three flight dates. The corresponding average change in the flux for the three flight dates was 23 % and 19 % for $CO_2$ and $CH_4$, respectively, with the largest change in the flux for the 1 March flight experiment (Table 2). This significant uncertainty is expected in part because the CBL depth increased without a corresponding increase in measurement transects to constrain the interpolation of the data up to the new CBL depth.

We determined the influence of the observed uncertainty in the perpendicular wind speed to the estimated flux, and found that changing the magnitude of the perpendicular wind speed by the overall uncertainty (~ 0.7 m s$^{-1}$), given the observed variability and the method uncertainty, yielded identical results for both the $CO_2$ and $CH_4$ fluxes (an average of 15 % and 17 % change in the flux for $CO_2$ and $CH_4$ respectively, at the





ACPD
13, 29895–29945, 2013



95 % CL, as shown in Table 2). We note that in addition to the impact of the wind variability on flux values, the history of the horizontal winds prior to the experiment can also be important in the mass balance approach. The presence of sustained, steady winds ensures that the integrated mass flux through the measurement plane at the time of measurement is essentially equal to the total mass flux from the source at the time of emission. The mean horizontal wind speeds were 5.8, 4.0, and 5.9 $m\,s^{-1}$ (averaged over all altitudes) for the 1 March, 29 April, and 1 June 2011 experiments, respectively. If the emissions from the city mix with an air mass traveling across Indianapolis with the observed wind speeds ($\sim$ 6 and 4 $m\,s^{-1}$), this air mass will pass from the city (taken to be $\sim$ 70 km wide) center to the point of interception in $\sim$ 1.5 to 2.5 h. This then is the required corresponding time frame for constant wind speeds, for a city of this size.

We calculated the variability in the gridded background concentrations at each 20 m altitude bin and determined the uncertainty introduced in the flux, as described above. On average, we obtained a change in the flux of 21 % for both $CO_2$ and $CH_4$ (Table 2). It is important to note that the uncertainty in the flux due to the background depends significantly on the magnitude of the enhancements. For large source strengths, such as power plants and landfills (e.g. Harding Street power plant and Southside landfill), the plume is clearly defined and easily detectable above background. Conversely, uncertainty in the background becomes more important for sources with smaller incremental enhancements (e.g. the distributed mobile source sector) above the background.

Given our procedure for acquisition of background data, the aircraft-based approach is sensitive to incremental enhancements from sources that are directly upwind of the city. Thus, sampling of the air mass concentrations directly upwind of the city across its horizontal width could help quantify the impact of direct upwind sources. Future use of both upwind aircraft-based measurements and ground-based measurements from upwind towers will also help reduce the impact of background concentration uncertainty.

We note that the sensitivity analyses discussed here do not necessarily capture all parameters influencing the accuracy of the flux determination. The interpolated $CO_2$ and $CH_4$ plumes in Fig. 4, for example, are not the result of a frozen field; that is,





ACPD
13, 29895–29945, 2013



they are observed images of the $CO_2$ and $CH_4$ plumes that will move spatially over a three-hour time period, the approximate duration of one flight experiment. This problem is amplified when the sampling distance is close to the source and not achieving well-mixed conditions. On the other hand, the impact of the background subtraction is smaller with a larger detected enhancement, reflecting a trade-off in errors. Thus, a component of the overall uncertainty not directly probed here is the impact of non-stationary plumes on the interpolation. Indirectly, this is reflected in the assessment of precision, as discussed below. However, the analysis presented here provides insights on procedures to improve the experimental approach, as discussed in Sect. 4.

### 3.4 Evaluation of method precision using measurements from multiple downwind distances

Here we discuss the results from four flight experiments that were designed to determine the precision of the approach. Using the multi-transect kriging approach, we calculated the flux from two or more downwind distances, and quantified the difference in the flux estimates, as a measure of the method precision.

#### 3.4.1 Newton County landfill experiments

Two flight experiments were conducted downwind of the Newton County landfill. Fig. S6 (Supplement) shows the flight paths for the 16 June 2011 and 3 May 2012 experiments. During the 16 June experiments, winds were from the west with an average magnitude of $8\,m\,s^{-1}$ and measurements were conducted at two downwind distances (5 and 11 km). On 3 May 2012, winds were from the southwest with an average magnitude of $11\,m\,s^{-1}$, and measurements were conducted at 11 and 16 km downwind distances. For the latter flight date, the horizontal transect measurements 16 km from the main source were also intercepting the plume of 7 dairy farms that were downwind of the landfill. These dairy farms were located between 11 and 16 km and hence, did not impact the 11 km measurements (Fig. S6, Supplement). A list of confined animal





ACPD
13, 29895–29945, 2013



feeding operations in Indiana (http://www.in.gov/idem/4994.htm, accessed 6 September 2012) shows that there were a total of 29 060 cattle and 6200 calves from the 7 dairy farms, from which we can estimate emissions.

In Fig. 7, we show the measured methane concentrations from the Newton County landfill experiments, for the 3 May 2012 measurement. We observed significant enhancements within the methane plume downwind of the landfill. The $CH_4$ background was 1850 ± 2 ppb while the enhancements were at least 100 ppb, but in some cases up to 400 ppb above the background. Because the ratio of the uncertainty in the background to the enhancement is small (≤∼ 2 %), the total uncertainty is minimized, and the plume is clearly defined, which then makes the comparison of the results for the two distances idealized. In this experiment, we note again that the observed methane plumes were not uniformly distributed in the vertical direction, and a well-mixed boundary layer could not be assumed.

Table 3 shows the estimated fluxes for the two Newton County landfill experiments and the percentage difference between fluxes for the two downwind distances. Because we were intercepting the plume from seven dairy farms during the 3 May 2012 experiment at 16 km downwind distance, we accounted for the contribution from a total of 35 260 dairy cattle and calves and subtracted their calculated emission from the total observed flux. We used emission factors derived from a tracer technique in the literature (Johnson et al., 1994; Westberg et al., 2001) to obtain the methane flux contribution from the dairy farms. Observed variability in repeated measurements over five days using the tracer technique was ±30 % (Johnson et al., 1994). The total estimated emission flux from the 16 km downwind distance was 108 mol $s^{-1}$ while the calculated methane flux from the dairy farms was 9 mol $s^{-1}$. The difference (99 mol $s^{-1}$) is the net emission from the landfill (Table 3). Based on the results shown in Table 3, the percentage differences in the methane fluxes for the two distances for the 16 June 2011 and 3 May 2012 experiments were 39 % and 20 %, respectively.





ACPD
13, 29895–29945, 2013



### 3.4.2 Twin Bridges landfill experiment

On 30 August 2012, we sampled the methane plume from the Twin Bridges Landfill using two sets of horizontal transects at 3 and 6 km downwind distances (Fig. S6, Supplement). Winds were from the southeast with an average magnitude of 5 m s$^{-1}$. Similar to the observations from the Newton Co Landfill experiments, the measured methane horizontal distributions from the Twin Bridges landfill show the plume to be clearly defined above the background with average enhancements of ∼ 150 ppb for the two downwind distances. We find that the methane fluxes were 16 mol s$^{-1}$ and 18 mol s$^{-1}$ corresponding to the 3 km and 6 km downwind distances (Table 3), respectively. These results represent, on average, a ∼ 12 % difference between the estimated fluxes.

### 3.4.3 Harding Street power plant experiment

Three sets of horizontal transects were conducted in rapid succession downwind of the Harding Street power plant on 1 June 2012 at 5, 8 and 17 km (Fig. S6, Supplement). The winds were from the northwest with an average magnitude of ∼ 10 m s$^{-1}$. This sampling day was characterized by dense cloud cover (boundary layer top clouds) and relatively high winds. During such days when aircraft vertical profiles through the top of the boundary layer are not possible (to protect the BAT probe), the depth of the boundary layer was estimated from the observed cloud base altitude (640 m a.g.l.). Table 3 shows the calculated fluxes from the three downwind distances. The average $CO_2$ flux from the three sets of transects was 1530 ± 790 mol s$^{-1}$, yielding a (1 standard deviation) precision of 52 %. Thus, based on the summary shown in Table 3, the lower and upper bounds of the precision determinations, for point sources, were 12 % and 52 %, with an average of ∼30 %.

Ideally, under steady conditions (e.g. steady, sustained winds and boundary layer depth, and constant emission from the source), the emission fluxes calculated from measurements at multiple downwind distances are essentially identical. Thus, the vari-





ACPD
13, 29895–29945, 2013



ability in the observed emission fluxes effectively quantifies the combined influences of various variables (meteorological conditions, sampling statistics, and instrumental limitations) that may affect the magnitude of the measured fluxes, and is therefore, a measure of the method precision. We can compare these results, which are at the low end of those reported by previous studies that made use of an aircraft-based mass balance approach to estimate emissions from an urban plume or an area-wide source for different trace gases: 20 % for CO and 40 % for $NO_x$ emissions from Augsburg, Germany (Kalthoff et al., 2002), 50 % for $CH_4$ from a pastoral farming region in New Zealand (Wratt et al., 2001), 50 % for $CH_4$ from dairy farms in the South Coast Air Basin, CA, USA (Pieschl et al., 2013), 100 % for $CO_2$ from Sacramento, CA, USA (Turnbull et al., 2011) and 100 % for $NO_x$ emission measurements from Birmingham, AL, USA (Trainer et al., 1995). In these previous studies, main sources of uncertainties in emission estimates were attributed to uncertainties in concentration measurements (Wratt et al., 2011), and variability of horizontal wind speeds (Trainer et al., 1995; Turnbull et al., 2011).

Figure 8 shows the 1 June 2012 $CO_2$ emissions from the Harding St. power plant estimated using the mass balance approach and those reported from stack measurements (EPA Air Markets Program Data: http://ampd.epa.gov/ampd/, accessed August 2012). For comparison, the HSPP $CO_2$ measured and reported emissions for 1 March, 29 April, and 1 June 2011 were also included (Fig. 8 and Table 1). To isolate the HSPP contribution from the total city emission, we assume that the plume cells are attributable to HSPP if the concentration is at least two standard deviations greater than the mean city concentration and that the back trajectory from the point of observation intersects with the power plant. Error bars in the mass balance approach represent a conservative 50 % (rounded off to the tens place) estimate, consistent with the relative uncertainty observed in the flux estimates from the three downwind distances during the 1 June 2012 HSPP experiment. The uncertainty in the reported stack measurements is estimated to be 29 %, which represents the standard deviation of the bias-corrected distribution of differences between the EPA CAMD and EIA (Energy In-





ACPD
13, 29895–29945, 2013



formation Administration) data on a monthly/yearly level for all power plant facilities in the United States. We observed that the emissions from the two approaches were not statistically significantly different for the 2011 flight experiments within the estimated uncertainties. However, the observed $CO_2$ flux on 1 June 2012 was 60 % smaller than reported by EPA. It is possible that the aircraft-based approach under-sampled the plume on this flight date because visual flight rules require that aircraft fly at least 150 m below the cloud cover. Nevertheless, it is possible to determine from this set of observations the contribution of the HSPP to the total citywide $CO_2$ flux. In Table 1, we summarize the isolated HSPP and citywide $CO_2$ emissions and determine from observations that the HSPP $CO_2$ flux accounts for ~ 54 % of the $CO_2$ emissions from the city, on average, for three afternoons in 2011. This result is larger than the findings (~ 37 %) of Mays et al. (2009). For comparison, Gurney et al. (2012) estimate a 28 % contribution from the HSPP power plant using the bottom-up approach for year 2002. Using the results from the HSPP $CO_2$ flux determined from the continuous stack monitoring for the three days considered in the analyses (Table 1), the HSPP $CO_2$ emissions contribute 34 % on average compared to the total citywide Hestia estimated flux (Table 1).

### 3.5 Evaluation of the single-transect mass-balance method

We revisited the 1 March, 29 April, and 1 June 2011 Indianapolis flight experiments and recalculated the fluxes using the single-transect mass-balance method. Several aircraft-based mass balance studies conducted to date have utilized a single-transect approach that assumes a uniformly mixed boundary layer for the enhancements (Karion et al., 2013b; Pieschl et al., 2013; Turnbull et al., 2011; Trainer et al., 1995; White et al., 1983). To evaluate the relative viability of such an approach, enabling more rapid flux measurements, we calculated the $CO_2$ and $CH_4$ emission fluxes using observations from each transect in our experiment days to obtain multiple independent estimates of the citywide flux for the 1 March, 29 April, and 1 June 2011 flight experiments. Table 4 shows the total number of transects sampled for each of the three flight dates as well as the number of usable transects for the single transect calculations.





ACPD
13, 29895–29945, 2013



To remove biases arising from the background, we used the mean of the background concentrations from the edges of the interpolated data (outside the city limits) corresponding to the altitudes of the individual transects. This approach is chosen since, when implementing a single transect approach, one would design a flight plan to ensure that adequate background data were acquired to support each sample transect. The perpendicular wind speed used in the calculation was the average wind speed normal to each transect. Table 4 shows the mean $CO_2$ and $CH_4$ emission fluxes for the three flight dates estimated using the single transect approach together with the relative standard deviation, which reflects the precision of the assumption that any given transect represents the full boundary layer in the vertical scale. For the case of the 1 March flight experiment, we present the percentage difference of the flux estimates from two transects. Table S4 (Supplement) shows all of the independently determined values of the $CO_2$ and $CH_4$ fluxes for the three flight dates. For comparison, Table 4 also shows the results from the multi-transect kriging method (also shown in Table 1). Precision for the multi-transect kriging method was taken as 30 % based on the average variability observed from the multiple downwind distance experiments (discussed in Sect. 3.4). We note that the precision for our multi-transect kriging method may be larger than this, given the larger scale and smaller incremental concentrations that apply to the urban scale measurements. We find that the estimated fluxes from the two approaches are not statistically significantly different if we compare the mean from the single transect approach. However, many individual determinations from the single transect approach (i.e. the way it would be implemented) would be significantly different from the multi-transect result. The variability of the determined fluxes from the single-transect approach range from 23 % to 65 %. We have shown in Fig. 6 the $CO_2$ and $CH_4$ observations for the 7 transects on 29 April 2011, for which we calculated a standard deviation of 51 % and 58 % for $CO_2$ and $CH_4$, respectively. The dashed lines represent the limits of integration in the horizontal direction corresponding to the city boundary. Based on the observed significant variability in the measured concentrations for the various transects as a function of altitude, it is not unexpected that the independently





ACPD
13, 29895–29945, 2013



determined fluxes were also highly variable. We show in Figs. 4 and S8 (Supplement) the corresponding horizontal transect observations for the 1 June and 1 March 2011 flight experiments, respectively. We note the strong methane signal measured in one horizontal transect but not observed in the other transects during the 1 March flight experiment (Fig. S8, Supplement). The result from this investigation indicates that the boundary layer is not always uniformly distributed during sampling. Our results indicated that to enable reliable uncertainty determinations, one would generally need to prove, through measurements in each case, that the boundary layer is well-mixed. However, doing so would then effectively remove the time-savings benefit of the single transect approach.

## 4 Conclusions

This research involved assessment of important variables contributing to the uncertainty of an aircraft-based mass balance approach. This uncertainty analysis is approach-dependent, e.g. on the method for acquiring background data, the number of transects, the distance from the sources, etc. The aircraft-based mass balance approach is an attractive method for quantifying emissions from both citywide and area-wide sources because of its inherent ability to cover the entire footprint of the source and its capability to determine the state of the boundary layer during measurement. Optimization of the experimental design is important, and one of the primary objectives of INFLUX. We suggest the following improvements in the method based on this study. Measurement performance improvements can be realized by (1) carefully determining the background $CO_2$ and $CH_4$ concentrations, (2) monitoring the dynamics of the convective boundary layer, and (3) increasing the number of downwind horizontal transect measurements. An upwind horizontal transect in the middle of the boundary layer to ascertain the background $CO_2$ and $CH_4$ concentrations would improve our approach, as the concentrations at the edges of the transects may not fully represent the background inflow into the city. Measurement in an upwind horizontal transect would then enable





ACPD
13, 29895–29945, 2013



the use of shorter and thus more transects downwind of the city with lengths sufficient to just encompass the approximate width of the plume from the city. Improved plume representation will result from increasing the number of downwind horizontal transects at multiple altitudes. To realize that benefit, it may be necessary, however, to assume a vertically invariant background because time limitations might not allow for sampling the upwind plume at multiple altitudes. We note also that this approach is not ideal if the background is diurnally varying, e.g. when the biospheric impact is significant. Of course, this situation could be dramatically improved with two aircrafts operating simultaneously, upwind and downwind of the city, so that direct inflow is measured, along with any temporally varying character to that background air.

A second component of the uncertainty in the estimated flux arises from uncertainty in boundary layer height. Thus a vertical profile obtained before and after the experiment on the downwind side would help monitor the dynamics of the CBL. Alternatively, continuous remotely sensed measurements of the CBL depth such as those obtained from Lidar backscatter profiles would also help better constrain the growth or decay of the boundary layer during the course of the experiment, thereby improving the overall uncertainties. Such data might provide more flight time allocated to acquisition of more upwind background data. As shown here, the process of interpolation also introduces uncertainties in the budget calculation, especially in the limit of a small number of transects. Therefore, multiple horizontal transects will minimize interpolation-related uncertainties. That recommendation is best implemented with higher aircraft speed.

We also evaluated the precision of the approach by comparing measurements made in rapid succession over transects at multiple downwind distances from three point (or small area) sources with large strengths. We obtained relative differences ranging from 12 % to 52 %, with an average of ∼ 30 %. Given that these experiments were conducted downwind of sources with large source strengths and smaller areal footprints, and that there are likely significant systematic errors, e.g. related to plume sampling statistics, we thus conservatively estimate the overall uncertainty (precision plus systematic errors) for individual urban flux measurements as ±50 % (maximum relative





ACPD
13, 29895–29945, 2013



difference rounded off to the tens place). This is consistent with the average difference between our determinations of the HSPP flux, and the EPA CEMS data for the flight dates studied here.

We also compared the multi-transect kriging approach with results from single transect realizations of the flux, assuming a well-mixed boundary layer. Our results suggest that there is a trade-off between the necessary downwind distance for complete mixing, and the ratio of the enhancement to the uncertainty in the background concentration. Thus, we recommend that multiple transects through the boundary layer are pursued when possible. We observed that the variability of the estimated flux from the single transect method ranged from 23 % to 65 % which treats each transect as a single realization of the flux while the interpolation method treats all the data as a single realization and does not assume that there is complete mixing throughout the boundary layer.

To obtain an aircraft-based flux measurement with comparable uncertainties for larger urban regions (e.g. megacities), the same number of transects will be necessary over a time period where the emission flux does not significantly change. Thus, the required aircraft speed would need to scale with the relative size of the city. For example, the raster length for the Indianapolis experiments is 70 km, while it is $\sim$ 120 km for a megacity region such as the Los Angeles, CA basin. Thus, an aircraft with a cruise speed of $\sim 120\,\mathrm{m\,s^{-1}}$ ($\sim$ 245 kts) would enable a comparable result. This is just below the FAA maximum allowed cruise speed below 3 km altitude. Improved data coverage and simultaneous acquisition of background data for megacities such as Los Angeles, São Paolo, and Beijing will thus require simultaneous operation of at least two aircrafts.

**Supplementary material related to this article is available online at http://www.atmos-chem-phys-discuss.net/13/29895/2013/acpd-13-29895-2013-supplement.pdf.**

*Acknowledgements.* This research work is part of the Indianapolis Flux Experiment (INFLUX), which is funded by NIST. We also thank the Purdue University Jonathan Amy Facility for Chemi-





ACPD
13, 29895–29945, 2013



cal Instrumentation (JAFCI) for technical support in this project. Many thanks also go to Kuldeep Prasad of NIST for his helpful comments in this manuscript.

Disclaimer: Some commercial instruments are identified to represent the data sources accurately. Such identification does not imply recommendation or endorsement by the National Institute of Standards and Technology, nor does it imply that the equipment identified is necessarily the best available for the purpose.

## References

America's Largest Landfills – CNBC: available at: http://www.cnbc.com/id/39382002/America_s_Largest_Landfills (last access: 6 September 2013), 2012

Bergamachi, P., Krol, M., Meirink, J. F., Dentener, F., Segers, A., van Aardenne, J., Monni, S., Vermeulen, A. T., Schmidt, M., Ramonet, M., Yver, C., Meinhardt, F., Nisbet, E. G., Fisher, R. E., O'Doherty, S., and Dlugokencky, E. J.: Inverse modeling of European $CH_4$ emissions 2001–2006, J. Geophys. Res., 115, D22309, doi:10.1029/2010JD014180, 2010.

Boden, T. A., Marland, G., and Andres, R. J.: Global, Regional, and National Fossil-Fuel $CO_2$ Emissions, Carbon Dioxide Information Analysis Center, Oak Ridge National Laboratory, US Department of Energy, Oak Ridge, Tenn., USA doi:10.3334/CDIAC/00001_V2010, 2010.

Chen, H., Winderlich, J., Gerbig, C., Hoefer, A., Rella, C. W., Crosson, E. R., Van Pelt, A. D., Steinbach, J., Kolle, O., Beck, V., Daube, B. C., Gottlieb, E. W., Chow, V. Y., Santoni, G. W., and Wofsy, S. C.: High-accuracy continuous airborne measurements of greenhouse gases ($CO_2$ and $CH_4$) using the cavity ring-down spectroscopy (CRDS) technique, Atmos. Meas. Tech., 3, 375–386, doi:10.5194/amt-3-375-2010, 2010.

Chu, D.: The GLOBEC kriging software package – EasyKrig3.0; Available from http://globec.whoi.edu/software/kriging/easy_krig/easy_krig.html, (last access: 20 January 2011) 2004.

Ciais, P., Paris, J., Marland, G., Peylin, P., Piao, S., Levin, I., Pregger, T., Scholz, Y., Friedrich, R., Houwelling, S., and Schulze, D.: The European carbon balance revisited, Part 1: Fossil fuel emissions, Glob. Change Biol., 16, 1395–1408, doi:10.1111/j.1365-2486.2009.02098.x, 2010.

Clyde, M. and George, E. I.: Model uncertainty, Stat. Sci., 19, 81–94, 2004.





ACPD
13, 29895–29945, 2013



Crosson, E. R.: A cavity ring-down analyzer for measuring atmospheric levels of methane, carbon dioxide, and water vapor, Appl. Phys. B-Lasers O., 92, 403–408, 2008.
Conway, T. J., Tans, P. P., Waterman, L. S., Thoning, K. W., Kitzis, D. R., Masarie, K. A., and Zhang, N.: Evidence for interannual variability of the carbon cycle from the NOAA/CMDL global air sampling network, J. Geophys. Res., 99, 22831–22855, 1994.
Dlugokencky, E. J., Masarie, K. A., Lang, P. M., Tans, P. P., Steele, L. P., and Nisbet, E. G.: A dramatic decrease in the growth rate of atmospheric methane in the Northern Hemisphere during 1992, Geophys. Res. Lett., 21, 45–48, 1994.
Dlugokencky, E. J., Myers, R., Lang, P., Masarie, K., Crotwell, A., Thoning, K., Hall B., Elkins, J., and Steele, L. P.: Conversion of NOAA/CMDL atmospheric dry air $CH_4$ mole fractions to a gravimetrically prepared standard scale, J. Geophys. Res., 110, D18306, doi:10.1029/2005JD006035, 2005.
Draxler, R. R. and Rolph, G. D.: HYSPLIT (HYbrid Single-Particle Lagrangian Integrated Trajectory) Model access via NOAA ARL READY Website (http://ready.arl.noaa.gov/HYSPLIT.php), NOAA Air Resources Laboratory, Silver Spring, MD, 2012.
Fan, J. and Gijbels, I.: Local Polynomial Modeling and Its Applications, Chapman and Hall, London, UK, 1996.
Forster, P., Ramaswamy, V. Artaxo, P., Berntsen, T., Betts, R., Fahey, D. W., Haywood, J., Lean, J., Lowe, D. C., Myhre, G., Nganga, J., Prinn, R., Raga, G., Schulz, M., and Van Dorland, R.: Changes in atmospheric constituents and in radiative forcing, in: Climate Change 2007: The Physical Science Basis, Contribution of Working Group I to the Fourth Assessment Report of the Intergovernmental Panel on ClimateChange, edited by: Solomon, S., Qin, D., Manning, M., Chen, Z., Marquis, M., Averyt, K. B., Tignor, M., and Miller, H. L., Cambridge University Press, Cambridge, UK, New York, NY, USA, 129–234, 2007.
Garman, K. E.: Precision of airborne wind measurement for atmospheric flight research, Ph.D. thesis, Purdue University, West Lafayette, Indiana, USA, 2009.
Garman, K. E., Hill, K. A., and Wyss, P., Carlsen, M., Zimmerman, J. R., Stirm, B. H., Carney, T. Q., Santini, R., and Shepson, P. B.: An airborne and wind tunnel evaluation of a wind turbulence measurement system for aircraft-based flux measurements, J. Atmos. Ocean. Tech., 23, 1696–1708, 2006.
Garman, K. E., Wyss, P., Carlsen, M., Zimmerman, J. R., Stirm, B. H., Carney, T. Q., Santini, R., and Shepson, P. B.: The contribution of variability of lift-induced upwash to the uncertainty





ACPD
13, 29895–29945, 2013



in vertical winds determined from an aircraft platform, Bound.-Lay. Meteorol., 126, 461–476, 2008.
Gregg, J. S., Andres, R. J., and Marland, G.: China: emissions pattern of the world leader in $CO_2$ emissions from fossil fuel consumption and cement production, Geophys. Res. Lett., 35, L08806, doi:10.1029/2007GL032887, 2008.
Guan, D., Liu, Z., Geng, Y., Lindner, S., and Hubacek, K.: The gigatonne gap in China's carbon dioxide inventories, Nature Clim. Change, 2, 672–675, doi:10.1038/nclimate1560, 2012.
Gurney, K. R., Mendoza, D. L., Zhou, Y., Fischer, M. L., Miller, C. C., Geethakumar, S., and de la Rue du Can, S.: High resolution fossil fuel combustion $CO_2$ emission fluxes for the United States, Environ. Sci. Technol., 43, 5535–5541, doi:10.1021/es900806c, 2009.
Gurney, K. R., Razlivanov, I., Song, Y., Zhou, Y., Benes, B., and Abdul-Massih, M.: Quantification of fossil fuel $CO_2$ emissions at the building/street level scale for a large U.S. city, Environ. Sci. Technol., 46, 12194–12202, doi:10.1021/es3011282, 2012.
Helman, C.: America's Biggest Landfills, available at: http://www.forbes.com/2010/10/13/los-angeles-las-vegas-business-energy-biggest-landfills.html (last access: 6 September 2013), 2012.
International Energy Agency: World Energy Outlook, 2008, IEA, Paris, France, 2008.
Indiana Department of Environmental Management Confined Feeding Operations: available at: http://www.in.gov/idem/4994.htm (last access: 6 September 2013), 2012.
Johnson, K., Huyler, M., Westberg, H., Lamb, B., and Zimmerman, P.: Measurement of methane emissions from ruminant livestock using a $SF_6$ tracer technique, Environ. Sci. Technol., 28, 359–362, 1994.
Kalthoff, N., Corsmeier, U., Schmidt, K., Kottmeier, Ch., Fiedler, F., Habram, M., and Slemr, F.: Emissions of the city of Augsburg determined using the mass balance method, Atmos. Environ., 36, S19–S31, 2002.
Karion, A., Sweeney, C., Wolter, S., Newberger, T., Chen, H., Andrews, A., Kofler, J., Neff, D., and Tans, P.: Long-term greenhouse gas measurements from aircraft, Atmos. Meas. Tech., 6, 511–526, doi:10.5194/amt-6-511-2013, 2013a.
Karion, A., Sweeney, C., Petron, G., Frost, G., Hardesty, R. M., Kofler, J., Miller, B. R., Newberger, T., Wolter, S., Banta, R., Brewer, A., Dlugokencky, E., Lang, P., Montzka, S. A., Schnell R., Tans, P., Trainer, M., Zamora, R., and Conley, S.: Methane emissions estimate from airborne measurements over a western United States natural gas field, Geophys. Res. Lett., 40, 1–5, doi:10.1002/grl.50811, 2013b.





ACPD
13, 29895–29945, 2013



Kort, E. A., Frankenberg, C., Miller, C. E., and Oda, T.: Space-based observations of megacity carbon dioxide, Geophys. Res. Lett., 39, L17806, doi:10.1029/2012GL052738, 2012.
Lafferty, J. and Wasserman, L.: Rodeo: sparse, greedy nonparametric regression, Ann. Stat., 36, 28–63, 2008.
Lenschow, D. H. and Stankov, B. B.: Length scales in the convective boundary layer, J. Atmos. Sci., 43, 1198–1209, 1986.
Marland, G.: Uncertainties in accounting for $CO_2$ from fossil fuels, J. Ind. Ecol., 12, 136–139, doi:10.1111/j.1530-9290.2008.00014.x, 2008.
Marland, G.: China's uncertain $CO_2$ emissions, Nature Clim. Change, 2, 645–646, 2012.
Mays, K. L., Shepson, P. B., Stirm, B. H., Karion, A., Sweeney, C., and Gurney, K. R.: Aircraft-based measurements of the carbon footprint of Indianapolis, Environ. Sci. Technol., 43, 7816–7823, 2009.
McKain, K., Wofsy, S. C., Nehrkorn, T., Eluszkiewicz, J., Ehleringer, J. R., and Stephens, B. B.: Assessment of ground-based atmospheric observations for verification of greenhouse gas emissions from an urban region, P. Natl. Acad. Sci. USA, 109, 8423–8428, doi:10.1073/pnas.1116645109, 2012.
Montzka, S. A., Myers, R. C., Butler, J. H., Elkins, J. W., and Cummings, S.: Global tropospheric distribution and calibration scale of HCFC-22, Geophys. Res. Lett., 20, 703–706, 1993.
Peters, G. P., Marland, G., Le Quere, C., Boden, R., Canadell, J. G., and Raupach, M. R.: Rapid growth in $CO_2$ emissions after the 2008–2009 global financial crisis, Nature Clim. Change, 2, 2–4, 2012.
Peylin, P., Houweling, S., Krol, M. C., Karstens, U., Rödenbeck, C., Geels, C., Vermeulen, A., Badawy, B., Aulagnier, C., Pregger, T., Delage, F., Pieterse, G., Ciais, P., and Heimann, M.: Importance of fossil fuel emission uncertainties over Europe for $CO_2$ modeling: model inter-comparison, Atmos. Chem. Phys., 11, 6607–6622, doi:10.5194/acp-11-6607-2011, 2011.
Peischl, J., Ryerson, T. B., Brioude, J., Aikin, K. C., Andrews, A. E., Atlas, E., Blake, D., Daube, B. C., de Gouw, J. A., Dlugokencky, E., Frost, G. J., Gentner, D. R., Gilman, J. B., Goldstein, A. H., Harley, R. A., Holloway, J. S., Kofler, J., Kuster, W. C., Lang, P. M., Novelli, P. C., Santoni, G. W., Trainer, M., Wofsy, S. C., and Parish, D. D.: Quantifying sources of methane using light alkanes in the Los Angeles basin, California, J. Geophys. Res. Atmos., 118, 1–17, doi:10.1002/jgrd.50413, 2013.
Ryerson, T. B., Trainer, M., Holloway, J. S., Parrish, D. D., Huey, L. G., Sueper, D. T., Frost, G. J., Donnelly, S. G., Schauffler, S., Atlas, E. L., Kuster, W. C., Goldan, P. D.,





ACPD
13, 29895–29945, 2013



Hubler, G., Meagher, J. F., and Fehsenfeld, F. C.: Observations of ozone formation in power plant plumes and implications for ozone control strategies, Science, 292, 719–723, doi:10.1126/science.1058113, 2001.
Samarov, D. V.: The Fast Rodeo for Local Polynomial Regression, Technical Report, National Institute of Standards and Technology, Gaithersburg, Maryland, USA, 2012.
Solid Waste Facility Annual Report for the State of Indiana: available at: http://www.in.gov/idem/files/solid_waste_fdr08.pdf (last access: 15 May 2011), 2008.
Stull, R. B.: An Introduction to Boundary Layer Meteorology, Kluwer Academic Publishers, Dordrecht, the Netherlands, 1997.
Trainer, M., Ridley, B. A., Buhr, M. P., Kok, G., Walega, J., Hubler, G., Parrish, D. D., and Fehsenfeld, F. C.: Regional ozone and urban plumes in the southeastern United States: Birminghan, a case study, J. Geophys. Res., 100, 18823–18834, 1995.
Turnbull, J. C., Lehman, S. J., Morgan, S., and Wolak, C.: A new automated extraction system for $^{14}C$ measurement in atmospheric $CO_2$, Radiocarbon, 52, 1261–1269, 2010.
Turnbull, J. C., Karion, A., Fischer, M. L., Faloona, I., Guilderson, T., Lehman, S. J., Miller, B. R., Miller, J. B., Montzka, S., Sherwood, T., Saripalli, S., Sweeney, C., and Tans, P. P.: Assessment of fossil fuel carbon dioxide and other anthropogenic trace gas emissions from airborne measurements over Sacramento, California in spring 2009, Atmos. Chem. Phys., 11, 705–721, doi:10.5194/acp-11-705-2011, 2011.
Turnbull, J. C., et al.: Atmospheric measurements of urban fossil fuel $CO_2$ emissions from the INFLUX experiment: effects of sampling location and choice of background, in preparation, 2013.
Vaughn, B. H., Ferretti, D. F., Miller, J. B., and White, J. W. C.: Stable isotope measurements of atmospheric $CO_2$ and $CH_4$, in: Handbook of Stable Isotope Analytical Techniques, Elsevier BV, Amsterdam, the Netherlands, 272–304, 2004.
Walter, D., Heue, K.-P., Rauthe-Schoch, A., Brenninkmeijer, C. A. M., Lamsal, L. N., Krotkov, N. A., and Platt, U.: Flux calculations using CARIBIC DOAS aircraft measurements: $SO_2$ emission of Norilsk, J. Geophys. Res., 117, D11305, doi:10.1029/2011JD017335, 2012.
Westberg, H., Lamb, B., Johnson, K. A., and Huyler, M.: Inventory of methane emissions from US cattle, J. Geophys. Res., 106, 12633–12642, 2001.
White, W. H., Patternson, D. E., and Wilson Jr., W. E.: Urban exports to the nonurban troposphere: results from project MISTT, J. Geophys. Res., 88, 10745–10752, 1983.





ACPD
13, 29895–29945, 2013



World Bank: Cities and Climate Change: an Urgent Agenda, Vol. 10, Washington, D.C., USA, 2010.
Wratt, D. S., Gimson, N. R., Brailsford, G. W., Lassey, K. R., Bromley, A. M., and Bell, M. J.: Estimating regional methane emissions from agriculture using aircraft measurements of concentration profiles, Atmos. Environ., 35, 497–508, 2001.
Wunch, D., Wennberg. P. O., Toon, G. C., Keppel-Aleks, G., and Yavin, Y. G.: Emissions of greenhouse gases from a North American megacity, Geophys. Res. Lett., 36, L15810, doi:10.1029/2009GL039825, 2009.
United States Environmental Protection Agency Greenhouse Gas Data: available at: http://ghgdata.epa.gov/ghgp/main.do (last access: 4 September 2012), 2012.
United States Environmental Protection Agency Air Markets Program Data: available at: http:10//ampd.epa.gov/ampd/ (last access: 24 August, 2012), 2013.
Zhao, C. L. and Tans, P. P.: Estimating uncertainty of the WMO mole fraction scale for carbon dioxide in air, J. Geophys. Res., 111, D08S09, doi:10.1029/2005JD006003, 2006.





ACPD
13, 29895–29945, 2013



**Table 1.** Citywide $CO_2$ and $CH_4$ emissions estimated from the aircraft-based mass balance approach and the Hestia bottom-up method corresponding to the three flight dates. Total uncertainty in the Hestia county-level emissions is (−15 %, +20 % at 95 % CL). Also shown are the Harding Street power plant (HSPP) $CO_2$ emissions from the mass balance approach and EPA stack measurements, and the mass balance HSPP percentage contribution to the total citywide $CO_2$ flux for the three flight dates. Uncertainty in the HSPP stack monitoring is 29 %.

| Flight Date in 2011 | Total city $CO_2$ Flux (mol $s^{-1}$) | Hestia fossil $CO_2$ flux (mol $s^{-1}$) | Total city $CH_4$ Flux (mol $s^{-1}$) | HSPP $CO_2$ Flux Mass Balance (mol $s^{-1}$) | HSPP $CO_2$ from EPA (mol $s^{-1}$) | % HSPP Contribution Mass Balance |
|---|---|---|---|---|---|---|
| 1 Mar | 11 000 | 12 122 | 93 | 5950 | 3589 | 54 |
| 29 Apr | 7500 | 10 751 | 101 | 5100 | 3871 | 68 |
| 1 Jun | 26 000 | 12 134 | 197 | 10 030 | 4407 | 39 |





ACPD
13, 29895–29945, 2013



**Table 2.** Percent change in (A) $CO_2$ and (B) $CH_4$ flux as a function of the uncertainties in analysis parameters for three Indianapolis flight dates in 2011.

| | (A) $CO_2$ Flux Sensitivity | | | |
|---|---|---|---|---|
| | 1 Mar | 29 Apr | 1 Jun | Average |
| Background | 13 | 18 | 31 | 21 ± 9 |
| CBL Depth | 32 | 22 | 14 | 23 ± 9 |
| Perpendicular Wind speed | 12 | 20 | 14 | 15 ± 4 |
| Interpolation Method | 0.2 | 28 | 9 | 12 ± 14 |
| | (B) $CH_4$ Flux Sensitivity | | | |
| | 1 Mar | 29 Apr | 1 Jun | Average |
| Background | 8 | 23 | 32 | 21 ± 12 |
| CBL Depth | 35 | 13 | 8 | 19 ± 14 |
| Perpendicular Wind speed | 12 | 21 | 17 | 17 ± 5 |
| Interpolation Method | 6 | 12 | 7 | 8 ± 3 |





ACPD
13, 29895–29945, 2013



**Table 3.** Percentage difference between estimated fluxes from two or more downwind distances for four flight experiments.

| Flight Date and Experiment | Downwind distance (km) | Flux ($mol\,s^{-1}$) | Difference (%) |
|---|---|---|---|
| 16 Jun 2011, Newton Co. Landfill ($CH_4$) | 5<br>11 | 56<br>83 | 39 |
| 3 May 2012, Newton Co. Landfill ($CH_4$) | 11<br>16 | 81<br>99 | 20 |
| 30 Aug 2012, Twin Bridges Landfill ($CH_4$) | 3<br>6 | 16<br>18 | 12 |
| 1 Jun 2012, Harding St. Power Plant ($CO_2$) | 5<br>8<br>17 | 1350<br>850<br>2400 | 52* |

* Derived from the standard deviation of the resulting $CO_2$ emission fluxes from the three downwind distances divided by the mean.





ACPD
13, 29895–29945, 2013



**Table 4.** Citywide $CO_2$ and $CH_4$ emission fluxes ($mol\,s^{-1}$) derived from the single transect method (mean ±1 s) and via the multi-transect kriging approach for the three flight dates in 2011. Percentage values in parenthesis represent the relative standard deviation. The stated precision in the multi-transect kriging approach is 30 %, the average precision obtained from the multiple downwind experiments (Table 3).

| Flight Date in 2011 | Total No. of Transects | No. of Usable Transects | Single Transect Method | | Multi-Transect kriging Approach | |
|---|---|---|---|---|---|---|
| | | | $CO_2$ Flux | $CH_4$ Flux | $CO_2$ Flux | $CH_4$ Flux |
| 1 Mar | 4 | 2 | 12 800 (17 000, 8700)[a] (65 %)[b] | 130 (170, 85)[a] (65 %)[b] | 11 000 ± 3300 | 93 ± 28 |
| 29 Apr | 7 | 5 | 8950 ± 4600 (51 %) | 105 ± 60 (58 %) | 7500 ± 2250 | 101 ± 30 |
| 1 Jun | 7 | 5 | 24 000 ± 5500 (23 %) | 190 ± 79 (42 %) | 26 000 ± 7800 | 197 ± 59 |

[a] Values of the flux estimates from the two individual transects.
[b] Represents the percentage difference between the flux estimates from the two individual transects.





ACPD
13, 29895–29945, 2013



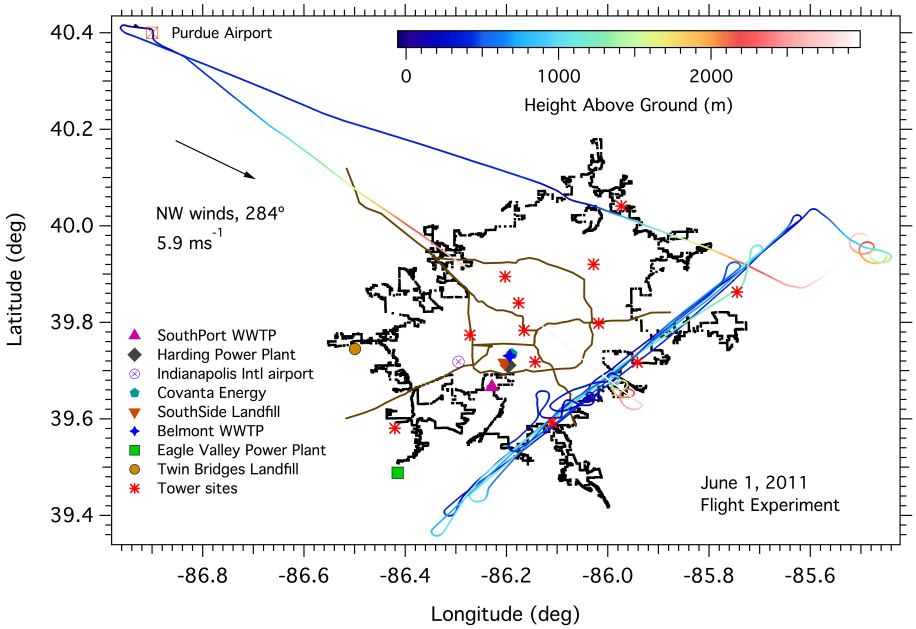


**Fig. 1.** Flight path as a function of altitude downwind of Indianapolis, IN USA on 1 June 2011. Mean winds were from the northwest at $\sim 6\,m\,s^{-1}$. Also shown are the locations of $CO_2$ and $CH_4$ sources within and around the city limits such as power plants (Harding Street and Eagle Valley power generating facilities), landfills, incineration plant (Covanta Energy), and wastewater treatment plants (Belmont WWTP and Southport WWTP). The brown outline represents the major highways inside the city.





ACPD
13, 29895–29945, 2013



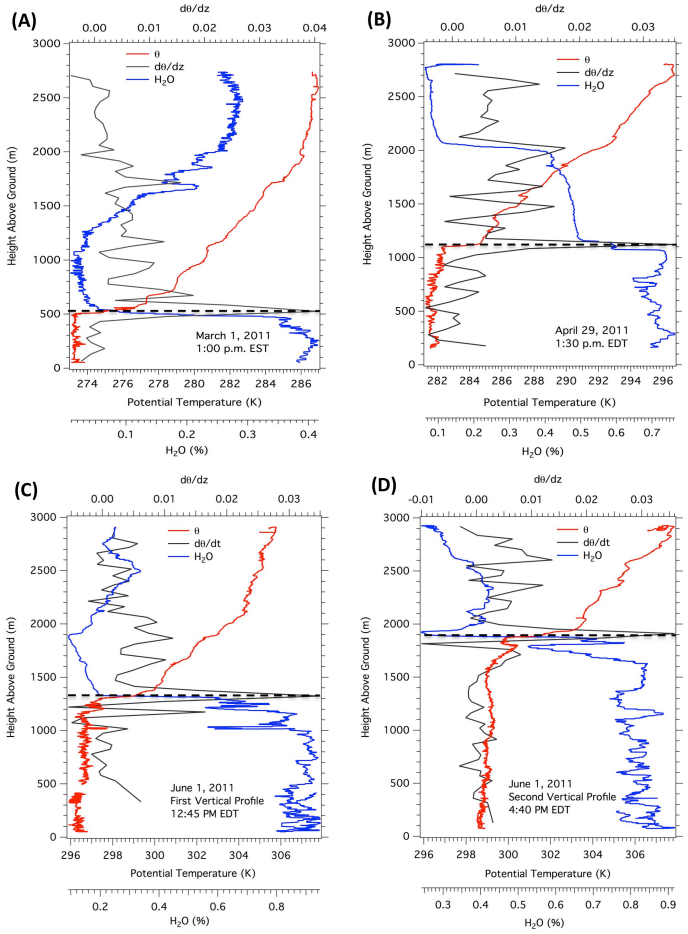


**Fig. 2.** Vertical ascending profiles of $H_2O$, potential temperature ($\theta$) and its gradient with altitude (d$\theta$/dz) for **(A)** 1 March, **(B)** 29 April; and **(C)** 1 June 2011 before, and **(D)** after the horizontal transects. Broken lines indicate the estimated CBL depths for the three flight experiments.





ACPD
13, 29895–29945, 2013



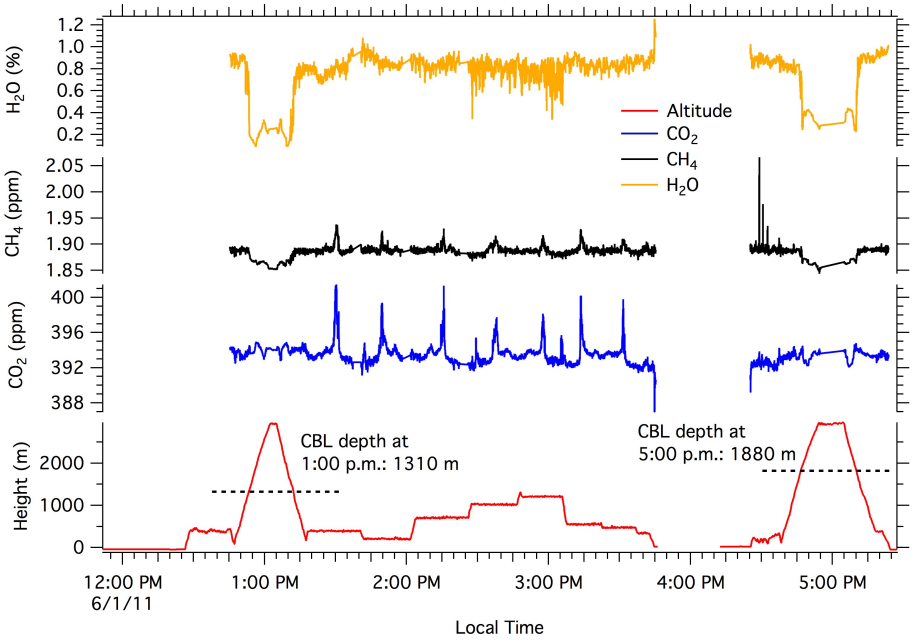


**Fig. 3.** Temporal distribution of altitude (m a.g.l.), carbon dioxide, methane and water on 1 June 2011. Two vertical profiles were performed during this flight experiment, showing a ~ 570 m growth in the boundary layer depth from the beginning of the experiment.





ACPD
13, 29895–29945, 2013



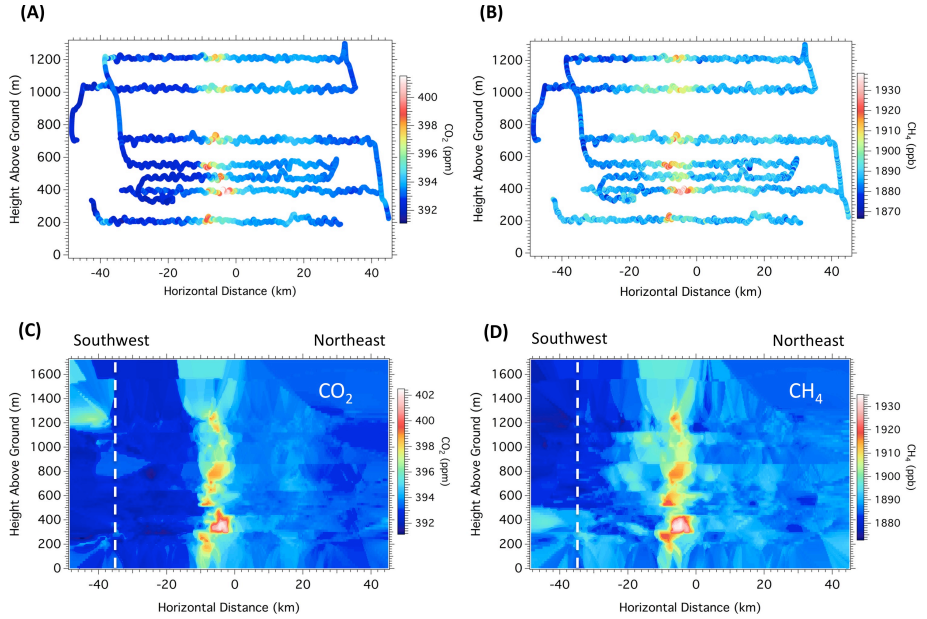


**Fig. 4.** Horizontal and vertical distributions of **(A)** observed $CO_2$, **(B)** observed $CH_4$, **(C)** kriged $CO_2$, and **(D)** kriged $CH_4$ on 1 June 2011 corresponding to the transects in Fig. 1. The northeast end corresponds to positive distances while the southwest end corresponds to negative distances relative to the chosen center point. The projected city limits were from −35 km (broken line) to +45 km. CBL depth was 1720 m.





ACPD
13, 29895–29945, 2013



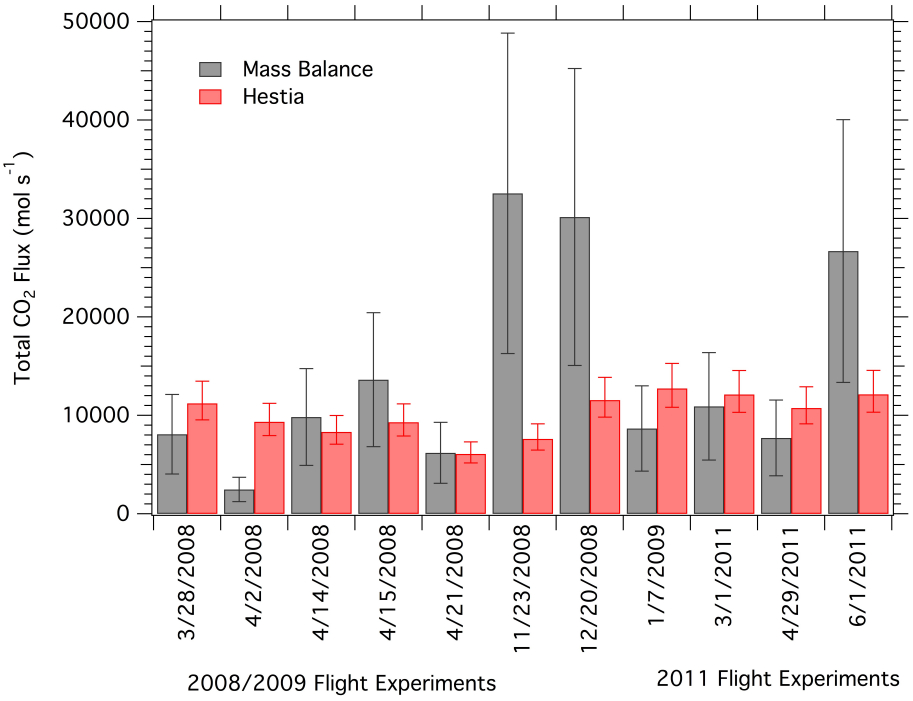


**Fig. 5.** Indianapolis $CO_2$ emissions for several flight experiments in 2008 and 2011 estimated from the aircraft-based mass balance and Hestia bottom-up approaches. Error bars in the mass balance approach represent our uncertainty estimate of ± 50 %, while the Hestia uncertainty is (−15 %, +20 %) at 95 % confidence interval for Marion county.





ACPD
13, 29895–29945, 2013



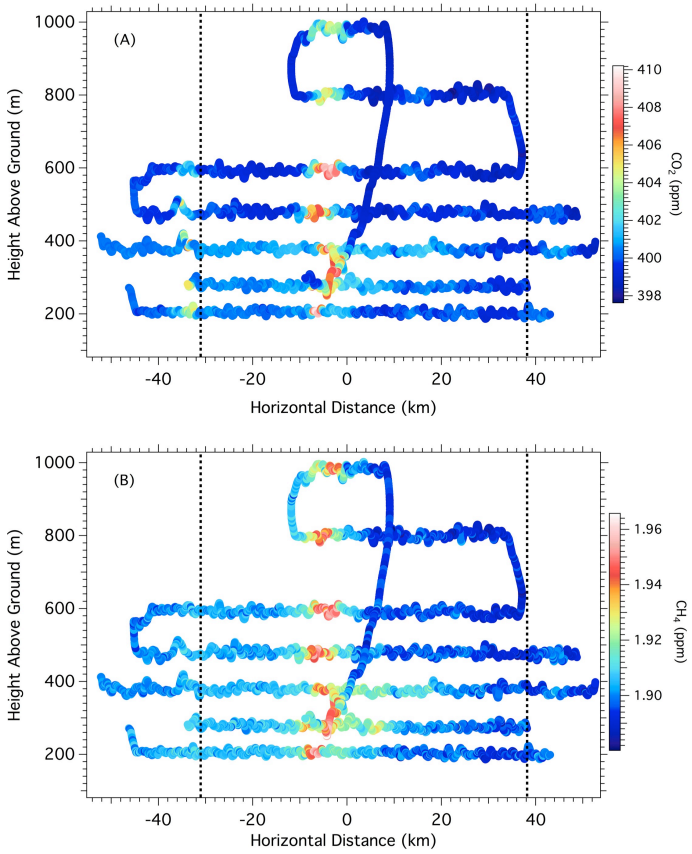


**Fig. 6. (A)** $CO_2$ and **(B)** $CH_4$ observations on 29 April 2011as a function of altitude and horizontal distance along the seven transects. Dashed lines represent the projected city limits. CBL depth was 1110 m.





ACPD
13, 29895–29945, 2013



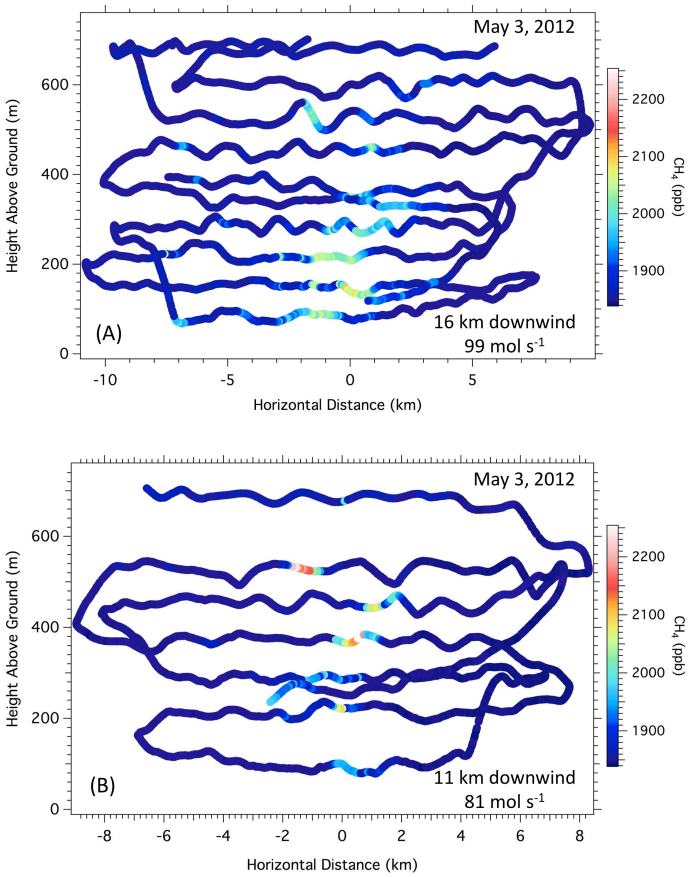


**Fig. 7.** Observed methane concentrations for the 3 May 2012 Newton Co. landfill flight experiment for two downwind distances **(A)** 16 km, and **(B)** 11 km. Vertical profiles were flown after the 16 km and 11 km horizontal transects, showing CBL depths of 700 m and 840 m, respectively.





ACPD
13, 29895–29945, 2013



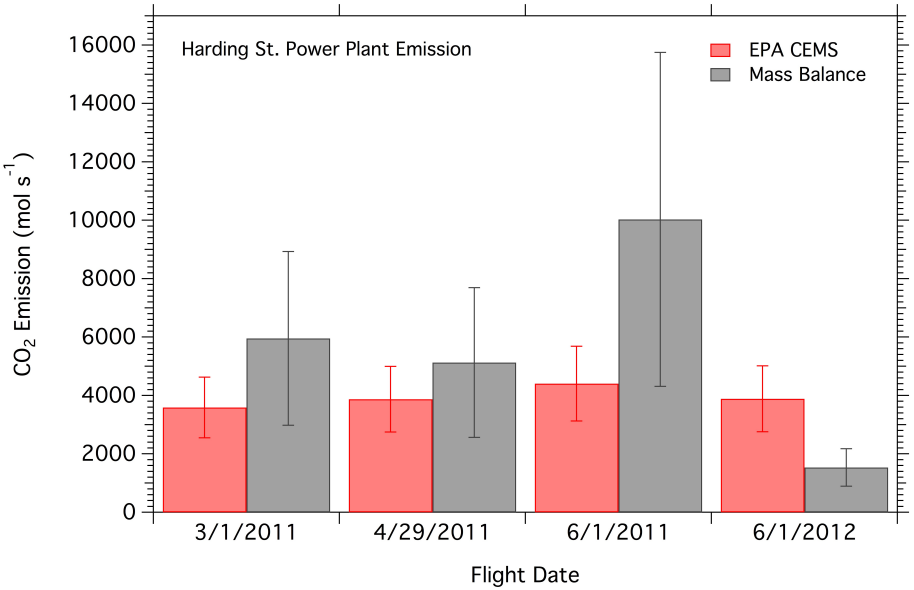


**Fig. 8.** Harding Street power plant $CO_2$ emission estimates from the mass balance and EPA CEMs monitoring approaches. Error bars in the CEMs monitoring represent a 29 % uncertainty while error bars in the mass balance approach correspond to the 50 % uncertainty estimate.





ACPD
13, 29895–29945, 2013